

THE (RE-)DISCOVERY OF G350.1–0.3: A YOUNG, LUMINOUS SUPERNOVA REMNANT AND ITS NEUTRON STAR

B. M. GAENSLER,^{1,8} A. TANNA,¹ P. O. SLANE,² C. L. BROGAN,³ J. D. GELFAND,^{4,9}
N. M. MCCLURE-GRIFFITHS,⁵ F. CAMILO,⁶ C.-Y. NG,¹ AND J. M. MILLER⁷

Accepted to *The Astrophysical Journal (Letters)*

ABSTRACT

We present an *XMM-Newton* observation of the long-overlooked radio source G350.1–0.3. The X-ray spectrum of G350.1–0.3 can be fit by a shocked plasma with two components: a high-temperature (1.5 keV) region with a low ionization time scale and enhanced abundances, plus a cooler (0.36 keV) component in ionization equilibrium and with solar abundances. The X-ray spectrum and the presence of non-thermal, polarized, radio emission together demonstrate that G350.1–0.3 is a young, luminous supernova remnant (SNR), for which archival H I and ¹²CO data indicate a distance of 4.5 kpc. The diameter of the source then implies an age of only ≈ 900 years. The SNR’s distorted appearance, small size and the presence of ¹²CO emission along the SNR’s eastern edge all indicate that the source is interacting with a complicated distribution of dense ambient material. An unresolved X-ray source, XMMU J172054.5–372652, is detected a few arcminutes west of the brightest SNR emission. The thermal X-ray spectrum and lack of any multi-wavelength counterpart suggest that this source is a neutron star associated with G350.1–0.3, most likely a “central compact object”, as seen coincident with other young SNRs such as Cassiopeia A.

Subject headings: ISM: individual (G350.1–0.3) — stars: neutron, individual (XMMU J172054.5–372652) — supernova remnants

1. INTRODUCTION

Many supernova remnants (SNRs) expand into complex environments shaped by molecular clouds and by the strong winds from OB associations. If our understanding of SNRs is to progress, we must aim to identify and understand these complicated systems.

G350.1–0.3 is a bright radio source in the inner Galaxy. Its linear polarization and non-thermal spectrum originally led to its classification as a SNR (Clark et al. 1973, 1975), but a high-resolution image (Salter et al. 1986) revealed a distorted, elongated, morphology, very different from the shell structure usually seen in such sources. Salter et al. (1986) argued that G350.1–0.3 was possibly a radio galaxy or a galaxy cluster. In subsequent SNR catalogs, the source was either downgraded to a SNR candidate or dropped completely (Green 1991; Whiteoak & Green 1996), and has subsequently been forgotten. We here present new and archival data on this unusual source. We demonstrate that G350.1–0.3 is a very young and luminous SNR expanding into dense ambient gas, and reveal an associated neutron star likely to be an addition to the growing class of “central compact objects” (CCOs).

2. OBSERVATIONS

In Figure 1(a) we show a 4.8 GHz radio image of G350.1–0.3, generated from Very Large Array (VLA) data taken in 1984 Jun 06 (C configuration; project code AV105), 1984

Aug 27 (D configuration; AV105) and 1989 Jun 23 (CnB configuration; AB544). The source is dominated by a bright double-peaked clump, with diffuse, elongated, structures extending to the north-east and north-west of this. G350.1–0.3 has been detected in X-ray surveys with *ROSAT* and *ASCA*, in which it was designated 1RXS J172106.9–372639 and AX J1721.0–3726, respectively (Voges et al. 1999; Sugizaki et al. 2001). These data provide limited spatial information (see Fig. 1[a]), but the ~ 1000 counts from *ASCA* are a good fit to a non-equilibrium ionization (NEI) plane-parallel shocked plasma with variable abundances (XSPEC model “VPSHOCK”; Borkowski et al. 2001), with absorbing column $N_H \approx 3 \times 10^{22} \text{ cm}^{-2}$, temperature $kT \approx 1.6 \text{ keV}$, an ionization time scale $\tau \approx 3 \times 10^{11} \text{ s cm}^{-3}$, an absorbed 0.5–10 keV flux $\approx 10^{-11} \text{ ergs cm}^{-2} \text{ s}^{-1}$, and enhanced levels of Si, S and Fe.

Data from the Southern Galactic Plane Survey (McClure-Griffiths et al. 2005) show that there is strong H I absorption seen against G350.1–0.3 at velocities in the range 0 to -40 km s^{-1} relative to the local standard of rest (LSR). However, no absorption is seen at -80 km s^{-1} , despite the presence of bright ($T \gtrsim 30 \text{ K}$) H I emission at this velocity and in this direction. The systemic velocity for G350.1–0.3 thus must fall in the range -80 to -40 km s^{-1} , ruling out an extragalactic origin and implying a distance¹⁰ between 4.5 and 10.7 kpc. In further discussion we adopt a distance to G350.1–0.3 of $4.5d_{4.5} \text{ kpc}$; in §4.1 we will argue that $d_{4.5} \approx 1$.

We observed G350.1–0.3 with *XMM-Newton* for 35 ks on 2007 Feb 23. The EPIC pn CCD was operated in full-frame mode, while EPIC MOS1 and MOS2 were used in large-window mode. The data were screened to remove hot pixels and flares, resulting in effective exposures of 34.7 ks (MOS) and 29.6 ks (pn).

3. RESULTS

¹⁰ We assume standard IAU parameters for the solar orbital velocity, $\Theta_0 = 220 \text{ km s}^{-1}$, and for the distance to the Galactic Center, $R_0 = 8.5 \text{ kpc}$.

¹ School of Physics, The University of Sydney, NSW 2006, Australia

² Harvard-Smithsonian Center for Astrophysics, Cambridge, MA 02138

³ National Radio Astronomy Observatory, Charlottesville, VA 22903

⁴ Center for Cosmology and Particle Physics, New York University, New York, NY 10023

⁵ CSIRO Australia Telescope National Facility, Marsfield, NSW 2122, Australia

⁶ Columbia Astrophysics Laboratory, Columbia University, New York, NY 10027

⁷ Department of Astronomy, University of Michigan, Ann Arbor, MI 48103

⁸ Australian Research Council Federation Fellow

⁹ Astronomy and Astrophysics Fellow, National Science Foundation

An *XMM* image of G350.1–0.3 is shown in Figure 1(b). Overall, the source is extremely bright: the background corrected count rates (0.5–10 keV) are 1.436 ± 0.007 counts s^{-1} (MOS1), 1.309 ± 0.007 counts s^{-1} (MOS2) and 2.97 ± 0.01 counts s^{-1} (pn), corresponding to $> 180\,000$ events from all three cameras combined. The source is dominated by a bright X-ray clump in the south-east, coincident with the region of brightest radio emission.

A notable difference between the two wavebands is the bright unresolved X-ray source $\approx 140''$ west of the brightest radio and X-ray emission. This source is at RA $17^{\text{h}}20^{\text{m}}54.^{\text{s}}5$, Decl. $-37^{\circ}26'52''$ (with an approximate uncertainty of $\pm 2''$ in each coordinate), and we correspondingly designate it XMMU J172054.5–372652. There is no radio counterpart in the VLA image, nor is there any optical or infrared source at this position in the Digitized Sky Survey, 2MASS or GLIMPSE. However, the optical and infrared limits are unconstraining given the heavy confusion and high extinction, along with the relatively large uncertainty of the *XMM* position.

3.1. Diffuse Emission

The X-ray spectrum of the brightest region, shown in Figure 2, is rich with line emission. No single thermal model can be sensibly fit to these data, but they can be adequately described by a two-component model, consisting of a low-temperature collisionally equilibrated plasma with solar abundances (XSPEC model “RAYMOND”; Raymond & Smith 1977), plus a higher-temperature component with a low ionization time scale (“VPSHOCK”) and with large over-abundances of all metals beyond neon (below which constraints cannot be obtained due to the large column density). The corresponding best joint fit to MOS1, MOS2 and pn data is shown in black in Figure 2 (only the pn spectrum is plotted), with parameters as listed in Table 1. Most of the significant residuals are below 1 keV, and indicate a problem with the model in the Fe-L region of the spectrum. An ad-hoc NEI model consisting only of an iron line (plus continuum) can further improve the fit, possibly suggesting a range of ionization time scales for Fe throughout the region. Spectra of the diffuse emission extending throughout the source are similar to that seen from the brightest region.

Even at the limited angular resolution of *XMM*, there is spectral structure within the brightest X-ray-emitting region. Extraction of separate sub-regions within this feature in circles of radius $12''$ reveal spectra that are each well-fit by a single absorbed VPSHOCK model, with temperatures and column densities consistent with those derived in Table 1 for the entire bright region. However, there are vast differences between regions in both abundances and ionization states. For example, a MOS1 spectrum from a $12''$ -radius circle centered at RA $17^{\text{h}}21^{\text{m}}07$, Decl. $-37^{\circ}26'46''$ (shown in red in Fig. 2) shows higher abundances in Si, Ar and Ca than emission $30''$ to the east of this (shown in blue in Fig. 2). Comparison of the He-like and H-like lines of Si indicates significant differences between the ionization levels of these two regions also.

3.2. The Compact Source

In contrast to the surrounding diffuse emission, the *XMM* spectrum of XMMU J172054.5–372652 shows a featureless continuum, as shown in green in Figure 2. These data cannot be described by the models considered in §3.1. An absorbed power law yields an acceptable fit ($\chi^2/\text{dof} = 1.16$) but with an unphysically steep photon index, $\Gamma = 5.4$. The best simple fit

($\chi^2/\text{dof} = 1.06$) is provided by an absorbed blackbody, with $N_H = (2.9 \pm 0.3) \times 10^{22}$ cm^{-2} , $kT = 0.53 \pm 0.02$ keV and an unabsorbed 0.5–10 keV flux $(1.4_{-0.4}^{+0.5}) \times 10^{-12}$ ergs cm^{-2} s^{-1} (errors all at 90% confidence).

The MOS data have a time-resolution of 0.9 s, while the pn events have a resolution of 73.4 ms. Within these constraints, we can search for X-ray pulsations from XMMU J172054.5–372652. We extracted 1378 MOS events and 922 pn events within $7''.5$ of the source and within the energy range 1–5 keV. The arrival times were shifted to the solar system barycenter, and a pulsation search was carried out using the Z_n^2 test (Buccheri et al. 1983). No significant periodic signals were found for $n = 1, 2, 3$. Assuming a sinusoidal pulse, the corresponding 99.999% confidence upper limits on the 1–5 keV pulsed fraction are $\sim 33\%$ for periods in the range 146 ms to 1.8 s, and $\sim 20\%$ for periods from 1.8 s up to 1 hour.

4. DISCUSSION

4.1. G350.1–0.3: A Young, Luminous SNR

G350.1–0.3 is extended, Galactic, and emits both polarized, non-thermal, radio emission and thermal X-rays with enhanced abundances. Despite its unusual morphology, its emission properties unquestionably demonstrate that it is a supernova remnant. The source diameter $D \approx 2.6d_{4.5}$ pc and unabsorbed 0.5–10 keV luminosity $L_X \approx 2d_{4.5}^2 \times 10^{36}$ ergs s^{-1} put this long over-looked source among the smallest and most luminous few SNRs in the Galaxy.

As is the case for other young SNRs (e.g., Lazendic et al. 2005; Morton et al. 2007), the high- and low-temperature components of the X-ray spectrum can be broadly interpreted as shocked ejecta and swept-up ambient material, respectively. The swept-up component has reached collisional equilibrium while the ejecta are still ionizing. The temperature of the ambient gas implies a shock velocity $V_s = 560_{-40}^{+20}$ km s^{-1} , assuming equilibration between ions and electrons. If we assume that the SNR is in the Sedov phase, we can estimate an age¹¹ $\text{age}_{\text{SNR}} = D/5V_s \approx 900d_{4.5}$ years, with the caveat that an accurate diameter is difficult to extract from the complex morphology.

Two independent calculations imply a high ambient density into which this SNR is expanding. First, the fact that the cooler shock component has reached collisional ionization equilibrium implies an ionization time scale $\tau \equiv n_e t_{\text{SNR}} \gtrsim 3 \times 10^{12}$ s cm^{-3} (Masai 1994; Borkowski et al. 2001), where n_e is the electron density of the swept-up material. This lower limit then implies an ambient density $n_0 \approx n_e/4 \gtrsim 25d_{4.5}^{-1}$ cm^{-3} . Second, standard Sedov expansion for $D = 2.6d_{4.5}$ pc and $t_{\text{SNR}} \approx 900d_{4.5}$ years implies $n_0/E_{51} \approx 600d_{4.5}^{-3}$ cm^{-3} , where $E_{51} \times 10^{51}$ ergs is the kinetic energy of the supernova explosion. For $E_{51} \approx 1$, the ambient density is again very high.

These results suggest that the SNR is interacting with dense, molecular, gas. The strange source morphology provides additional evidence for a molecular cloud interaction, since such encounters can produce SNRs with asymmetric and highly distorted appearances (e.g., Tenorio-Tagle et al. 1985; Wilner et al. 1998). In this case, the dense material is expected to sit east of the SNR, adjacent to the brightest radio/X-ray emission. Support for this conclusion is provided by the ^{12}CO survey of Bitran et al. (1997), which shows that immediately to the east of G350.1–0.3 is a clump of molecular gas at LSR velocity -40 km s^{-1} . We propose that G350.1–0.3

¹¹ If electron-ion equilibration has not yet been achieved, the true age is even lower than this estimate.

is associated with this cloud; the distance to the system is then 4.5 kpc, so that $d_{4.5} \approx 1$.

4.2. XMMU J172054.5–372652: A Candidate CCO

XMMU J172054.5–372652 is an unresolved thermal X-ray source with no radio counterpart, in close proximity to a young SNR. We thus suggest that this source is a neutron star associated with G350.1–0.3. This would require that G350.1–0.3 be the result of a core-collapse supernova (as also implied by the evidence for interaction with a molecular cloud, as discussed in §4.1). There are a wide variety of categories into which young neutron stars can fall. The absence of any non-thermal component to the X-ray spectrum of XMMU J172054.5–372652 rules out magnetospheric or nebular emission associated with a young, rotation-powered pulsar. Furthermore, while young pulsars can also show thermal surface emission, the blackbody temperature of these X-rays is typically $kT \lesssim 0.1$ keV, much lower than seen here (Kaspi et al. 2006).

The observed surface temperature $kT \approx 0.5$ keV and 0.5–10 keV luminosity $L_X \approx 3d_{4.5}^2 \times 10^{33}$ ergs s⁻¹ of XMMU J172054.5–372652 are both within the range seen for magnetars (Woods & Thompson 2006). However, the X-ray spectra of magnetars show hard power-law tails, unlike what is seen here. Magnetars show slow (~ 2 –12 sec) X-ray pulsations, often with a significant ($\gtrsim 40\%$) pulsed fraction. While the lack of slow pulses in our data provides initial evidence against such an identification, deeper pulsation searches will be needed to fully constrain such behavior. A more likely possibility is that XMMU J172054.5–372652 is a central compact object (see De Luca 2008, for a review). This group of ~ 10 sources are all associated with young SNRs. They are all thermal X-ray sources, with X-ray luminosities $\sim 10^{33}$ ergs s⁻¹, and blackbody temperatures $kT \approx 0.3$ –0.5 keV. Two CCOs are pulsed (at periods of 105 & 424 ms; Gotthelf & Halpern 2008); the rest show no X-ray variability. No CCOs show counterparts in other wavebands.

XMMU J172054.5–372652 appears to meet all these criteria; we thus propose that it is a CCO associated with G350.1–0.3. One potential difficulty with this claim is that within the formal statistical errors, the absorbing columns of the SNR and of the compact source are inconsistent. However, there is uncertainty as to the true spectral shape of both sources: in the case of the SNR because of unmodeled residuals in the spectrum below 1 keV, and for XMMU J172054.5–372652 as a result of likely atmospheric effects on the neutron star surface (which we have not attempted to fit for here). With these systematic effects included, the foreground columns of the two sources are sufficiently close that they can be considered consistent. In any case, the proposed interaction with molecular material may lead to large position-dependent fluctuations in absorption.

Other CCOs are found very close to the geometric centers of their associated SNRs. In contrast, XMMU J172054.5–372652 sits at the western extreme of the extended radio and X-ray emission, suggesting that it received a substantial kick in the supernova explosion. If we identify the centroid of the lowest radio contour in Figure 1 as the explosion site, the offset of the CCO from the SNR center is $\approx 2d_{4.5}$ pc, requiring a projected space velocity for the neutron star of ≈ 2000 km s⁻¹

(independent of $d_{4.5}$). We consider this unlikely, since this value is well above the 330 km s⁻¹ measured for the CCO in Cassiopeia A (Thorstensen et al. 2001), and exceeds even the 1100–1600 km s⁻¹ projected velocity measured for the CCO in Puppis A (Hui & Becker 2006; Winkler & Petre 2007). An alternative is that the CCO is still reasonably close to the site of the original supernova, and that a considerable portion of the SNR (farther to the west) remains unseen in both the radio and X-ray bands. Although there is a proposed molecular cloud interaction to the east, ejecta traveling westward may be expanding relatively unimpeded into a low density environment. Another possibility is that G350.1–0.3 is actually two or more overlapping or interacting SNRs (e.g., Williams et al. 1997), and that XMMU J172054.5–372652 is at the center of a partial shell corresponding to the fainter, western, half of the overall X-ray structure.

5. CONCLUSION

New X-ray data demonstrate that G350.1–0.3 is a very young (~ 900 year old) and luminous supernova remnant, most likely interacting with a molecular cloud at a distance of 4.5 kpc. We also identify the compact thermal X-ray source XMMU J172054.5–372652, which we propose as a central compact object associated with G350.1–0.3.

The complicated morphology and spectrum of the SNR make it difficult to carry out detailed calculations of its properties. For example, the spectrum of the diffuse emission that extends throughout the rest of the remnant is consistent with that from the brightest region, indicating that ejecta fills the X-ray emitting regions. However, this leaves open the question of why there is such a bright concentration in one small region of the SNR. Higher angular resolution observations of the SNR with the *Chandra X-ray Observatory*, combined with further millimeter observations of the environment into which the source is expanding, are needed to better address such issues. The nature of XMMU J172054.5–372652 also needs further confirmation — deeper *XMM* observations at high time resolution can provide better constraints on pulsations, while a subarcsecond localization from *Chandra* can enable a deep search for an infrared counterpart.

Clearly, G350.1–0.3 is one of a growing number of “missing” SNRs needed to balance the estimated supernova rate for the Milky Way of one per ~ 50 years. It is noteworthy that at least four such sources, G1.9+0.3 (Reynolds et al. 2008), G12.8–0.0 (Brogan et al. 2005), G327.2–0.1 (Gelfand & Gaensler 2007) and now G350.1–0.3, have all been recently revealed to be very young SNRs as a result of follow-ups to X-ray or γ -ray detections. Further investigation of unidentified Galactic high-energy sources will likely add further to this exciting sample of objects.

We thank John Hughes and Rob Fesen for helpful discussions, and the Lorentz Centre at Leiden University where some of this work was carried out. We acknowledge the support of NASA through grants NNX06AH60G & NAG5-13032 (B.M.G.) and contract NAS8-39073 (P.O.S.). NRAO is a facility of the NSF, operated under cooperative agreement by AUI.

Facilities: XMM (EPIC), VLA

REFERENCES

TABLE 1. SPECTRAL FIT OF A TWO-TEMPERATURE SHOCKED PLASMA TO THE REGION OF BRIGHTEST X-RAY EMISSION IN G350.1–0.3.

	VPSHOCK	RAYMOND
N_H^a	$3.71^{+0.05}_{-0.09} \times 10^{22} \text{ cm}^{-2}$	
kT (keV)	$1.46^{+0.09}_{-0.06}$	$0.36^{+0.02}_{-0.05}$
τ	$3.0^{+0.3}_{-0.4} \times 10^{11} \text{ s cm}^{-3}$...
Ne	40^{+70}_{-20}	(1)
Mg	20^{+140}_{-10}	(1)
Si	20^{+90}_{-10}	(1)
S	12^{+70}_{-5}	(1)
Ca	18^{+5}_{-7}	(1)
Fe	6^{+7}_{-3}	(1)
Flux ^b	$(6-14) \times 10^{-10} \text{ ergs cm}^{-2} \text{ s}^{-1}$	
χ^2/dof	1679/1135=1.48	

NOTE. — The three spectra from EPIC MOS1, MOS2 and pn were fit jointly to an absorbed VPSHOCK + RAYMOND spectral model, except for the overall normalization, which was fit independently for each instrument. Uncertainties are all statistical errors at 90% confidence, except for the unabsorbed flux, for which the range given reflects systematic uncertainties between the fluxes measured with MOS1, MOS2 and pn. Abundances are relative to solar; entries in parentheses indicate quantities held fixed at solar values.

^aInterstellar absorption has been calculated using the model of Wilms et al. (2000) assuming solar abundances, and has been applied simultaneously to both temperature components.

^bThe flux is the sum of both components over the energy range 0.5–10.0 keV, and has been corrected for foreground absorption.

- Brogan, C. L., et al. 2005, *ApJ*, 629, L105
 Buccheri, R., et al. 1983, *A&A*, 128, 245
 Clark, D. H., Caswell, J. L., & Green, A. J. 1973, *Nature*, 246, 28
 —. 1975, *Aust. J. Phys. Astr. Supp.*, 37, 1
 De Luca, A. 2008, in *40 Years of Pulsars: Millisecond Pulsars, Magnetars and More*, ed. C. Bassa, Z. Wang, A. Cumming, & V. M. Kaspi (New York: AIP), 311–319
 Gelfand, J. D. & Gaensler, B. M. 2007, *ApJ*, 667, 1111
 Gotthelf, E. V. & Halpern, J. P. 2008, in *40 Years of Pulsars: Millisecond Pulsars, Magnetars and More*, ed. C. Bassa, Z. Wang, A. Cumming, & V. M. Kaspi (New York: AIP), 320–324
 Green, D. A. 1991, *PASP*, 103, 209
 Hui, C. Y. & Becker, W. 2006, *A&A*, 457, L33
 Kaspi, V. M., Roberts, M. S. E., & Harding, A. K. 2006, in *Compact Stellar X-ray Sources*, ed. W. H. G. Lewin & M. van der Klis (Cambridge: Cambridge University Press), 279–339
 Lazendic, J. S., O., S. P., Hughes, J. P., Chen, Y., & Dame, T. M. 2005, *ApJ*, 618, 733
 Masai, K. 1994, *ApJ*, 437, 770
 McClure-Griffiths, N. M., Dickey, J. M., Gaensler, B. M., Green, A. J., Haverkorn, M., & Strasser, S. 2005, *ApJS*, 158, 178
 Morton, T. D., et al. 2007, *ApJ*, 667, 219
 Raymond, J. C. & Smith, B. W. 1977, *ApJS*, 35, 419
 Reynolds, S. P., Borkowski, K. J., Green, D. A., Hwang, U., Harrus, I., & Petre, R. 2008, *ApJ*, submitted (arXiv:0803.1487)
 Salter, C. J., Patnaik, A. R., Shaver, P. A., & Hunt, G. C. 1986, *A&A*, 162, 217
 Sugizaki, M., Mitsuda, K., Kaneda, H., Matsuzaki, K., Yamauchi, S., & Koyama, K. 2001, *ApJS*, 134, 77
 Tenorio-Tagle, G., Bodenheimer, P., & Yorke, H. W. 1985, *A&A*, 145, 70
 Thorstensen, J. R., Fesen, R. A., & van den Bergh, S. 2001, *AJ*, 122, 297
 Voges, W., et al. 1999, *A&A*, 349, 389
 Whiteoak, J. B. Z. & Green, A. J. 1996, *A&AS*, 118, 329
 Williams, R. M., et al. 1997, *ApJ*, 480, 618
 Wilms, J., Allen, A., & McCray, R. 2000, *ApJ*, 542, 914
 Wilner, D. J., Reynolds, S. P., & Moffett, D. A. 1998, *AJ*, 115, 247
 Winkler, P. F. & Petre, R. 2007, *ApJ*, 670, 635
 Woods, P. M. & Thompson, C. 2006, in *Compact Stellar X-ray Sources*, ed. W. H. G. Lewin & M. van der Klis (Cambridge: Cambridge University Press), 547–586

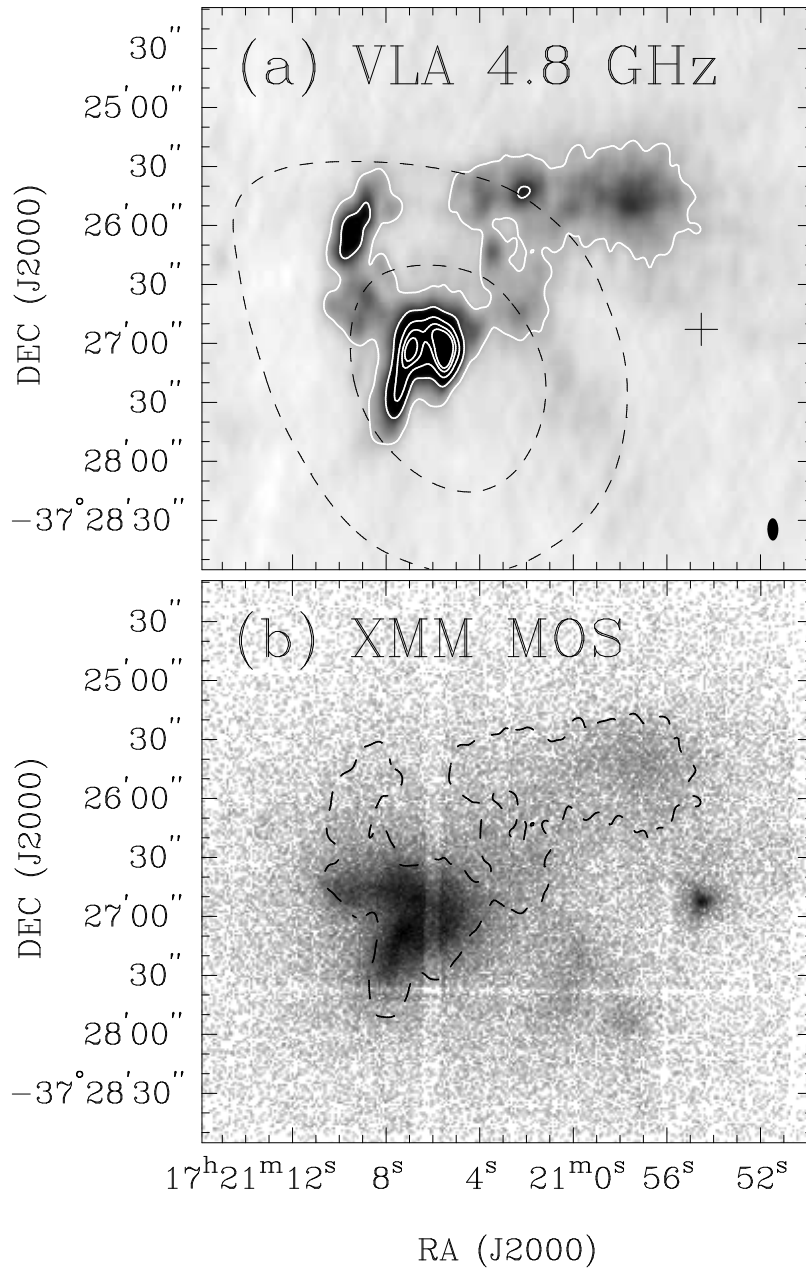


FIG. 1.— Radio and X-ray observations of G350.1-0.3. Panel (a) shows a 4.8 GHz image at a resolution of $11''.4 \times 5''.6$ (indicated by the ellipse at lower right) and a sensitivity of $170 \mu\text{Jy beam}^{-1}$, generated from archival VLA data. The greyscale is linear between -1 and $+10 \text{ mJy beam}^{-1}$; white contours are at levels of 2, 8, 16, 24 & 30 mJy beam^{-1} . The dashed contours show *ROSAT* All-Sky Survey data smoothed to $2'$ and with contours at 50% & 80% of the peak. The cross marks the position of XMMU J172054.5-372652. Panel (b) corresponds to the sum of *XMM* EPIC MOS1 and MOS2 data in the energy range 0.5-10 keV, with a logarithmic greyscale in units of counts. The dashed contour corresponds to the VLA data from panel (a) at the level of 2 mJy beam^{-1} .

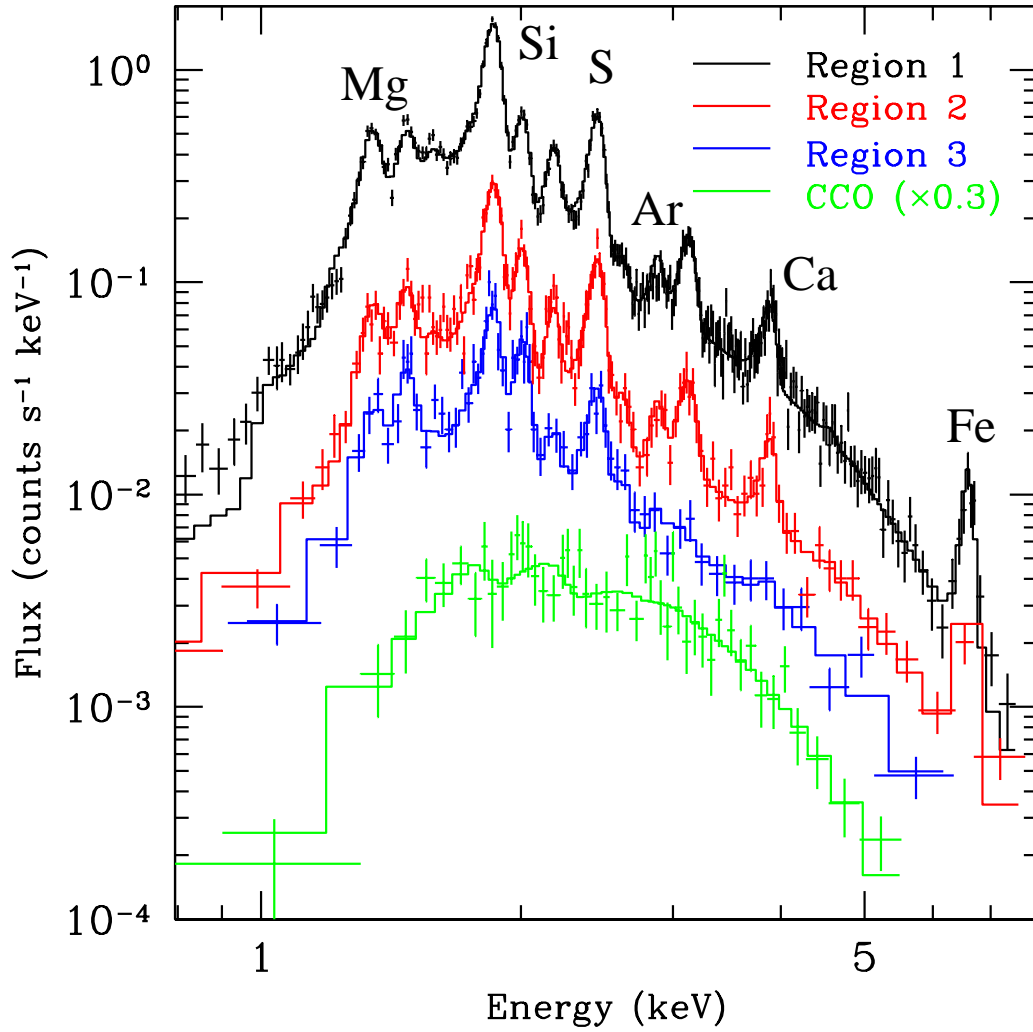


FIG. 2.— *XMM* spectra of G350.1–0.3. The black spectrum corresponds to EPIC pn data from the brightest diffuse region, extracted from a circle of radius $48''$, centered on (J2000) RA $17^{\text{h}}21^{\text{m}}07^{\text{s}}.44$, Decl. $-37^{\circ}27'01''.8$; several atomic emission lines are apparent, as indicated. The red and blue data show EPIC MOS1 spectra from two adjacent sub-regions within the region shown in black (see text for details). The green spectrum is that of EPIC pn data within a $21''$ -radius circle centered on the unresolved source XMMU J172054.5–372652. In all cases, the points show the data after appropriate background subtraction, while the solid lines represent the corresponding best-fit models as discussed in the text.